

Article ID: 1007-4627(2011)04-0416-07

Delta Excitation Calculation Studies in Compressed Finite Spherical Nucleus $^{40}\text{Ca}^*$

Mohammed H. E. Abu-Sei'leek

(Department of Physics, College of Sciences, Majmaah University, Zulfi, Kingdom of Saudi Arabia)

Abstract: With an oscillator basis, the nuclear Hamiltonian is defined in a no-core model space. It consists of an effective nucleon-nucleon interaction obtained with Brueckner theory from the Reid soft core interaction, a Coulomb potential, nucleon-delta transition potentials, and delta-delta interaction terms. By performing spherical Hartree-Fock (SHF) calculations with the realistic baryon Hamiltonian, the ground state properties of ^{40}Ca are studied. For an estimate of how the delta degree of freedom is excited, SHF calculations are performed with a radial constraint to compress the nucleus. The delta degree of freedom is gradually populated as the nucleus is compressed. The number of Δ 's is decreased by increasing model space. Large amount of the compressive energy is delivered to create massive Δ in the nucleus. There is a significant reduction in the static compression modulus for RSC static compressions which is reduced by including the Δ excitations. The static compression modulus is decreased significantly by enlarging the nucleon model space. The results suggest that inclusion of the delta in the nuclear dynamics could head to a significant softening of the nuclear equation of state.

Key words: nuclear structure; compressed finite nucleus; Δ -Resonance

CLC number: O571.2 **Document code:** A

1 Introduction

The nucleus is considered as a collection of nucleon (N) and delta (Δ) resonances interacting via realistic effective (N- Δ) interactions in a large but finite model space. The effect of including the Δ resonances on the Hartree-Fock energy (E_{HF}), Δ -orbital occupations, and radial density distribution is investigated under large amplitude state compression at temperature $T=0$.

In our earlier work, the excitation of Δ -degree of freedom in ^{40}Ca nucleus in constrained spherical Hartree-Fock(CSHF) was investigated^[1]. In Ref. [1], the ground state properties of ^{40}Ca nucleus was examined in small model space that consisted

from a six major oscillator shells for N and a six orbitals for Δ . The goal of this work is reexamined these properties of ^{40}Ca nucleus in large model space that consists of nine oscillator shells for N and ten orbitals for Δ .

The excitation of Δ isobars is very important to understand structure of nuclei at intermediate and high energies. It forms various probes to provide an exciting challenge both theoretically and experimentally, especially in the search for constructive, coherent pion production^[2-3]. The Δ excitation and its decay to nucleon and to pions are of current interest for understanding collision of light and heavy ions^[4-9].

This paper is organized as follows: Sec. 2

* **Received date:** 5 Jan. 2011; **Revised date:** 27 Feb. 2011

Biography: Mohammed H. E. Abu-Sei'leek (1972 -), male (Jordanian Nationality), Zarqa-Jordan, Assistant Professor Dr., working on Nuclear Structure Computational Physics; E-mail: moh2hassen@yahoo.com

specifies the definition of the nuclear Hamiltonian. The effective Hamiltonian used in the calculation is displayed in Sec. 3. The calculation procedure and strategy are outlined in Sec. 4. Results and discussions are presented in Sec. 5. Conclusions will be presented in Sec. 6.

2 Definition of the Nuclear Hamiltonian

The nuclear Hamiltonian that is coupled channels from a pure nucleon-nucleon (N-N) sector, a nucleon-delta (N- Δ), a Δ -nucleon (Δ -N) sector, and a (Δ - Δ) sector is

$$H = T - T_{c.m.} + V^{BB'} + V_C, \quad (1)$$

where T is a one-body kinetic energy term, $T_{c.m.}$ is the center of mass kinetic energy, $V^{BB'}$ the strong interaction between the baryons and V_C is Coulomb interaction. The nucleon mass is m , the delta mass is M and the speed of light $c=1$.

We define relative kinetic energy T_{rel} as:

$$T_{rel} = T - T_{c.m.} = \frac{\sum_{i < j} (\mathbf{p}_i - \mathbf{p}_j)^2}{2mA}, \quad (2)$$

with

$$T = \sum_{i=1}^A \left[\left(\frac{p_i^2}{2m} + m \right) \tau_{op_i}^{1/2} + \left(\frac{p_i^2}{2M} + M \right) \tau_{op_i}^{3/2} \right] \quad (3)$$

and

$$T_{c.m.} = \frac{p_{c.m.}^2}{2M_A} = \frac{1}{A} \sum_{ij} \frac{\mathbf{p}_i \cdot \mathbf{p}_j}{2m}, \quad (4)$$

where M_A is the total mass of nucleus, $M_A = mA$, p_i is the single particle momentum operator and τ_{op}^r is single particle isospin projection operator.

$$\tau_{op}^r | \tau' \rangle = \delta_{r\tau'} | \tau' \rangle, \quad (5)$$

$$\tau_{op}^{1/2} | \tau_{op}^{3/2} \rangle = 1, \quad (6)$$

the full Hamiltonian of the system can be written as the one-body and two-body parts as follows:

$$H_{eff} = H_1 (\text{one-body}) + H_2 (\text{two-body}), \quad (7)$$

where

$$H_1 (\text{one-body}) =$$

$$\left[\sum_{i=1}^A \frac{p_i^2}{2M} \left(\frac{m-M}{m} \right) + (M-m) \right] \tau_{op}^{3/2}, \quad (8)$$

and

$$H_2 (\text{two-body}) = T_{rel}(m) + V_{eff}^{BB'} + V_C. \quad (9)$$

H_1 arises due to the presence of the Δ 's. It consists of a mass correction and a kinetic energy term for the delta particles multiplied by a negative factor. These terms give non-zero contribution in Δ -sector only, since projection operator $\tau_{op}^{3/2}$ works in the space $\tau^{3/2}$ only.

H_2 is the effective baryon-baryon interaction that consists of the effective N-N interaction that was represented by Reid soft core (RSC) potential^[10] plus the transition potentials among baryons, which are generally labeled by $V_{\pi, \rho}^{B_1 B_2 \leftrightarrow B'_1 B'_2}$, where $B_1 B_2$ represent initial baryons and $B'_1 B'_2$ represent final baryons^[11]. The allowed exchanged mesons are π - and ρ -meson only. Other mesons do not contribute since they cannot change the spin and isospin of a nucleon to the value of 3/2 for the Δ isobar.

The effective two-baryon interaction is

$$V_{eff}^{BB'} = V_{\pi, \rho}^{NN \leftrightarrow NN} + V_{\pi, \rho}^{NN \leftrightarrow N\Delta} + V_{\pi, \rho}^{NN \leftrightarrow \Delta\Delta} + V_{\pi, \rho}^{N\Delta \leftrightarrow N\Delta} + V_{\pi, \rho}^{N\Delta \leftrightarrow \Delta N} + V_{\pi, \rho}^{N\Delta \leftrightarrow \Delta\Delta} + V_{\pi, \rho}^{\Delta\Delta \leftrightarrow \Delta\Delta}. \quad (10)$$

The explicit form of the resonance part of the transition potential read as:

$$V_{\pi, \rho}^{B_\alpha B_\beta \leftrightarrow B'_\alpha B'_\beta} = (\tau_{B_\alpha B_\beta}^1 \cdot \tau_{B'_\alpha B'_\beta}^2) \{ (\sigma_{B_\beta B'_\beta}^1 \cdot \sigma_{B_\alpha B'_\alpha}^2) \times [V_{c, \pi}^{B'_\alpha B'_\beta B_\beta B_\alpha} \cdot \pi(r) + 2V_{c, \rho}^{B'_\alpha B'_\beta B_\beta B_\alpha} \cdot \rho(r)] + S_{12}^{B'_\alpha B'_\beta B_\beta B_\alpha} \times [V_{T, \pi}^{B'_\alpha B'_\beta B_\beta B_\alpha} \cdot \pi(r) - V_{T, \rho}^{B'_\alpha B'_\beta B_\beta B_\alpha} \cdot \rho(r)] + \alpha_1 V_s^{B'_\alpha B'_\beta B_\beta B_\alpha} \cdot \rho(r) \} + \alpha_2 (1 \rightleftharpoons 2), \quad (11)$$

where $B_\alpha, \dots, B'_\beta$ denote nucleon or delta resonances, the function V_c, V_T , and V_s are the central, tensor, and spin part potentials respectively. For more detail see Ref. [1].

The Coulomb term, V_C , is taken to be the average Coulomb potential energy per proton and Δ^+ in a uniformly charged sphere

$$V_C = \frac{6}{5} \frac{Ze^2}{R} \left[1 - 5 \left(\frac{3}{16\pi Z} \right)^{2/3} - \frac{1}{Z} \right], \quad (12)$$

where Z is atomic number of nucleus, $Z^{-2/3}$ term is the exchange contribution and the Z^{-1} term sub-

tracts the interaction of the proton with itself and Δ^+ .

3 Effective Hamiltonian

By applying the variation principle, Hartree-Fock equation for nucleon and delta orbitals can be derived from the effective Hamiltonian with the chosen model space^[1].

In calculations, no-core oscillator model space that includes 9 major oscillator shells was used. In the 9 shells, 37 nucleon orbitals were used: $0s_{1/2}$, $0p_{3/2}$, $0p_{1/2}$, $0d_{5/2}$, $1s_{1/2}$, $0d_{3/2}$, $0f_{7/2}$, $1p_{3/2}$, $0f_{5/2}$, $1p_{1/2}$, $0g_{9/2}$, $1g_{7/2}$, $1d_{5/2}$, $1d_{3/2}$, $2s_{1/2}$, $0h_{11/2}$, $0h_{9/2}$, $1f_{7/2}$, $1f_{5/2}$, $2p_{3/2}$, $2p_{1/2}$, $0i_{13/2}$, $1g_{9/2}$, $2d_{5/2}$, $0i_{11/2}$, $1g_{7/2}$, $3s_{1/2}$, $2d_{3/2}$, $0j_{15/2}$, $0j_{13/2}$, $1h_{11/2}$, $1h_{9/2}$, $2f_{7/2}$, $2f_{5/2}$, $3p_{3/2}$, $3p_{1/2}$, $0k_{17/2}$ and for the delta states, 10 delta orbitals were used: $0p_{3/2}$, $0p_{1/2}$, $0d_{5/2}$, $0d_{3/2}$, $0f_{7/2}$, $0f_{5/2}$, $1p_{3/2}$, $1p_{1/2}$, $0g_{9/2}$, $0g_{7/2}$. A total of 47 baryon orbitals were included.

The matrix elements of the effective Hamiltonian had been calculated using the Brueckner G -matrix method^[12]. The effective N-N interaction was the sum of the Brueckner G -matrix and the lowest order fold diagram acting between pairs of nucleons in a no-core model space^[13–14]. RSC potential for the N-N interaction was adopted. To approximate the N-N interaction term of H_{eff} , the Brueckner G -matrix in an oscillator basis consisting of the lowest 9 oscillator shells using the methods of Refs. [13–15] is solved. Therefore, working in a no-core basis space, $\hbar\omega = 14$ MeV, and $\omega = 9$ MeV is used. The lowest order N-N folded diagram based on this G -matrix as described in Refs. [13–15] is added. This greatly reduces the ω -dependence of the N-N contribution to H_{eff} . In principle, if all folded diagram to all orders was incorporated, this ω -dependence would be eliminated completely^[16–18].

4 Calculation Procedure and Strategy

The used strategy is the same as in the earlier

studies^[1, 19–22]. It is summarized as following: First, the effective Hamiltonian in the nucleon sector only is considered (i. e. by turning off the (N- Δ) interaction). This is followed by calculating the ground state properties in the spherical Hartree-Fock (SHF) approximation (i. e. Hartree-Fock energy, E_{HF} , and the root mean square radius (r_{rms})) by adjusting the strength of the kinetic and potential factors in H_{eff} until agreement between SHF results, the experimental binding energy and experimental radius at equilibrium are obtained. The adjusting parameters λ_1 and λ_2 are introduced to adjust the matrix elements of T_{ref} and V_{eff} , respectively. Since the two-body matrix elements are evaluated with an oscillator energy spacing $\hbar\omega = 14$ MeV, these matrix elements are then scaled to the new oscillator basis characterized by a new value of $\hbar\omega'$ as described by Refs. [13–14, 23]. Second, the N- Δ and Δ -N interactions are activated. The adjusting parameters and $\hbar\omega'$ for ^{40}Ca nucleus in a given model space at equilibrium with the Δ channel turned off are obtained in Table 1. The binding energy (point mass r_{rms}) that was fitted was -342 MeV (3.46 fm) for ^{40}Ca . Third, the N- Δ and Δ -N interactions are turned off and a radial constraint $-\beta r^2$ is utilized to include the static compression. Where r is the one-body scalar radius operator. Fourth, the N- Δ and Δ -N interactions are activated and again, the radial constraint $-\beta r^2$ is applied and the difference in E_{HF} from the third step and current step as a function of r_{rms} is observed.

Table 1 Adjusting parameters λ_1 , λ_2 , and $\hbar\omega'$ of effective Hamiltonian for ^{40}Ca for the model space of nine oscillator shells for which the calculations were performed

Nucleus ^{40}Ca	λ_1	λ_2	$\hbar\omega'/\text{MeV}$
(9 shell)	0.999	1.093	11.700

5 Results and Discussion

In the previous studies^[1, 24–26], the following

quantities: The Hartree-Fock energy, the root mean square radius, the number of delta particles in the occupied orbitals, the radial density distribution, the single-particle energies, and the occupation probability of the single-particle orbitals were calculated in the case of small model space. In this work, more detailed results for ^{40}Ca nucleus are presented in order to examine its properties under static compression in a larger model space consisting of nine major oscillator shells (excluding $\ell > 5$) for nucleons and ten orbitals for Δ 's making a total of 47 baryons orbitals.

The Hartree-Fock energies E_{HF} versus r_{rms} using RSC potential are displayed in Fig. 1 for ^{40}Ca . The solid line represents the results of calculation performed in the nucleon-only sector and the dashed line represents the results obtained when the Δ 's are added in the ten orbitals: $0p_{3/2}$, $0p_{1/2}$, $0d_{5/2}$, $0d_{3/2}$, $0f_{7/2}$, $0f_{5/2}$, $1p_{3/2}$, $1p_{1/2}$, $0g_{9/2}$, $0g_{7/2}$. Note that, in the constrained SHF (CSHF) approximation, the nucleons and delta may only mix in the $0p_{3/2}$, $0p_{1/2}$, $0d_{5/2}$, $0d_{3/2}$, $0f_{7/2}$, $0f_{5/2}$, $1p_{3/2}$, $1p_{1/2}$, $0g_{9/2}$, and $0g_{7/2}$ states.

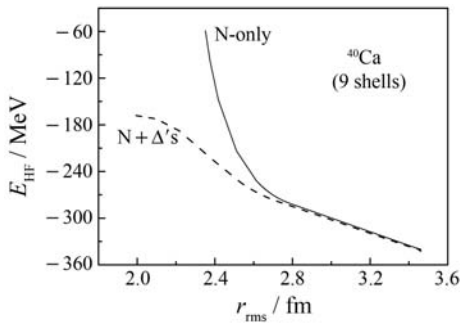


Fig. 1 CSHF energy as a function of the point mass r_{rms} for ^{40}Ca evaluated in 9 major oscillator shells with 10 Δ -orbitals.

Fig. 1 clearly shows that there is virtually no difference in the results with and without Δ 's at equilibrium. It is seen that without the Δ -degree of freedom in the system, E_{HF} increases steeply towards zero binding energy under compression. When the transition to Δ is allowed, the nucleus remains bound as density is increased to 5.26 of

normal density. Considering only the nucleons, the volume (based on the root mean square radius) of nucleus decreases by about 31%, the binding energy will be about 160.88 MeV with the inclusion of the Δ -excitations. In other words, this shows about 282.96, and 122.08 MeV of excitation energy to achieve a 31% volume reduction in the nucleon-only results, and nucleons and Δ^+ 's results, respectively.

It appears that from the above results, 122.08 MeV of excitation energy is enough to reduce the volume by 31% and the energy by 36% more. The results show that there is a significant reduction in the static compression modulus for RSC static compressions which is reduced by including the Δ excitations. The consequence of this reduction is a softening of the nuclear equation of state at larger compression. To see the role of Δ in determining the equation of state, Fig. 1 shows the dependence of the E_{HF} on the compression characterized by the r_{rms} . It can be seen that near equilibrium ($r_{\text{rms}} = 3.46$ fm) all curves agree. Also, the inclusion of Δ orbitals tends to decrease of E_{HF} for compressed nuclei. The role of the Δ 's is less significant as the r_{rms} approaches the ground state value.

Fig. 1 shows that as the static load force increases, the compression of nucleus with nucleons only is less than the other nucleus with nucleons and Δ 's.

The difference between the results of the Hartree-Fock binding energy obtained in this work and those in Refs. [1, 24–26] is the size of the nucleon model space, the number of the Δ orbitals included, different potentials and more compression, and also it is worth mentioning that at equilibrium (no constraint) in ^{40}Ca , it was not found any mixing between nucleon states and the Δ states. As same as in Refs. [1, 24–26], all curves of E_{HF} agree near equilibrium ($r_{\text{rms}} = 3.46$ fm). This implies that the results for the system at equilibrium don't depend on model space. In comparison with the results in previous studies [1, 24–26],

current results are consistent with the results obtained for ^{40}Ca for E_{HF} . The results of the Hartree-Fock energy without comparison and the behavior of curves for nucleons only and nucleons + Δ 's are the same for both the six and nine shells^[1]. The static compression modulus is decreased significantly by enlarging the nucleon model space. The current results display more compression than previous studies^[1, 24-26]. The results show that there is a significant reduction in the static compression modulus for RSC static compressions which are reduced by including the Δ excitations. The consequence of this reduction is a softening of the nuclear equation of state at larger compression.

In order to elucidate the role of the Δ 's as a function of compression, the number of Δ 's against r_{rms} radius was plotted in Fig. 2. The total number of Δ 's, the number of Δ^+ 's and Δ^0 's are plotted separately.

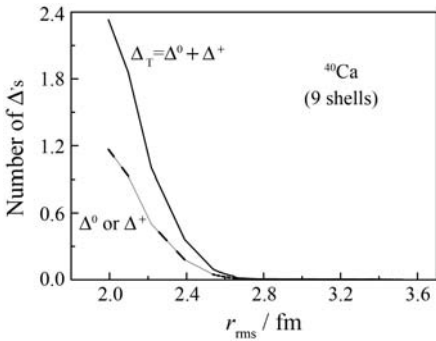


Fig. 2 Number of Δ 's as a function of r_{rms} for ^{40}Ca in 9 major shells model space. The upper curve is for the total number of Δ 's. The solid curve is for the number of Δ^+ , and the dashed curve is for Δ^0 .

In Fig. 2, the number of deltas increases rapidly as volume decreases. When the nucleus volume is reduced to about 81% of its volume at equilibrium, the number of deltas is increased to about 5.8% of all constituents of ^{40}Ca . It is interesting to note in Fig. 2 that the number of Δ^0 's and Δ^+ 's are the same. This is due to the fact that the number of neutrons is equal to the number of protons in ^{40}Ca nucleus.

Although there is a rapid rise of the Δ -population as compression increases, the change in the total number of Δ 's does not exceed 0.058 in Fig. 2. Is this a reasonable amount of Δ population? To examine this issue, it is interesting to note that there is a consistency of the amount of N- Δ mixing with the amount of excitation energy exhibited with compression. That is, for example, when 0.058 Δ 's are presented, the excitation energy is in the order of 0.058 $(M-m) \approx 17.23$ MeV. Thus, on the scale of the unperturbed single-particle energies (including the rest mass of the nucleons and deltas), a substantial fraction of the compressive energy is delivered, through the N- Δ and Δ - Δ interactions, to create more massive baryons in the lowest energy configuration of the nucleus. By other words, the number of Δ 's can be increased to about 2.33 at $r_{\text{rms}} = 1.99$ fm which corresponds to about 5.26 times the normal density.

Fig. 2 shows that the number of created Δ 's increases sharply, when ^{40}Ca nucleus compressed to a volume of about 0.81 of its equilibrium size. However, at this nuclear density, which is 5.26 times the normal density, the percentage of nucleons converted to Δ is only about 5.8% in ^{40}Ca .

The numbers of Δ^+ 's and Δ^0 's are the same for both the six and nine shell as shown in Fig. 2 in the present work and Ref. [1]. If one compare the current results of Fig. 2 with Fig. 8 of Ref. [25], then the number of Δ 's is decreased by increasing model space as seen from Table 2.

Table 2 The number of Δ 's is calculated with H_{eff} (RSC)

Number of	Ref. [25]	Our results
Δ 's is 0.09	(6 shells)	(9 shells)
r_{rms}/fm	3.26	2.55

One potential consequence of this result is that it could represent a collective mechanism for "Sub-threshold" pion production. That is, in "Sub-threshold" pion production experiments between

colliding nuclei where the bombarding energy per nucleon is below that needed to produce pions in N-N collisions. If the collisions produce isothermal compression, then the Δ 's are populated and relaxation could occur by decay of the Δ ' to a nucleon and a pion. These calculations support a collective mechanism for subthreshold pion production.

In the relativistic heavy-ion collisions, the nucleus that can more easily penetrate when the Δ degree of freedom becomes explicit is implied by Fig. 1. Because of the limitations of the model space, the calculations for higher densities are more speculative. Nevertheless it can give us some idea about how the Δ population can be increased as the nucleus is compressed to higher densities accessible to relativistic heavy-ion collisions. The results shown in Figs. 1 and 2 are consistent with the results extracted from relativistic heavy-ions collisions^[6-9].

Fig. 3 displays the radial density distributions of protons, neutrons, total radial density at equilibrium for ^{40}Ca state without any compression with point mass radius $r_{\text{rms}} = 3.46$ fm in a model space of nine major oscillator shells with Δ excitation restricted to the ten orbitals: $0p_{3/2}$, $0p_{1/2}$, $0d_{5/2}$, $0d_{3/2}$, $0f_{7/2}$, $0f_{5/2}$, $1p_{3/2}$, $1p_{1/2}$, $0g_{9/2}$, $0g_{7/2}$. It can be seen from this figure, there is no a radial density distribution for Δ at the ground state of ^{40}Ca nucleus without any compression. The radial density distributions have inverse relation with square of the radius.

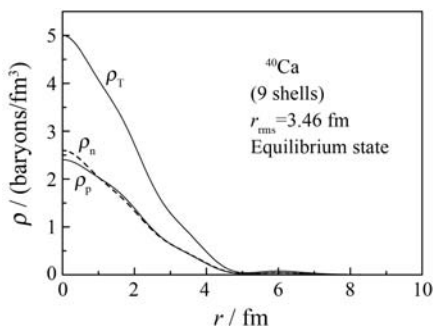


Fig. 3 Total ρ_T , proton ρ_p (solid line), and neutron ρ_n (dashed line) radial density distributions for ^{40}Ca at equilibrium state without any compression in a model space of nine major oscillator shells.

Fig. 4 shows the radial density distribution for neutrons ρ_n , protons ρ_p , deltas ρ_Δ , and their sum ρ_{TT} as a function of the radial distance from the center of the nucleus at large compression in a model space of nine major oscillator shells. The ρ_Δ is scaled by a factor of 5 to make it visible on the same scale as ρ_n and ρ_p . From this figure, the neutron radial density is higher than the proton density at all values of r . This is due to Coulomb repulsion between the protons. The Δ -radial density distribution, under high compression (point mass $r_{\text{rms}} = 2.54$ fm), reaches a peak value of about 0.01 of the proton (or neutron) radial density at $r = 2.20$ fm. Δ -mixing with the nucleons in the $0p_{3/2}$, $0p_{1/2}$, $0d_{5/2}$, $0d_{3/2}$, $0f_{7/2}$, $0f_{5/2}$, $1p_{3/2}$, $1p_{1/2}$, $0g_{9/2}$, and $0g_{7/2}$ orbitals occurs and this explains the shape of the Δ -radial distribution presented in Fig. 4.

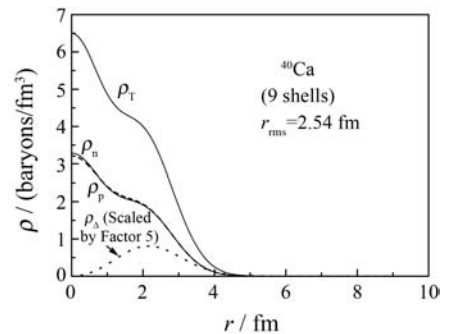


Fig. 4 Total ρ_T , proton ρ_p (dashed line), neutron ρ_n (solid line), and delta ρ_Δ (dotted line) radial density distributions for ^{40}Ca at point mass $r_{\text{rms}} = 2.54$ fm in a model space of nine major oscillator shells.

Fig. 5 displays the radial density distributions of ^{40}Ca evaluated at the about 0.19 reduced volume ($r_{\text{rms}} = 1.99$ fm). In this case, the Δ -radial density distribution reaches a peak value of about 0.26 of the proton radial density. The peak value of the radial density distribution for Δ appears at about 2 fm for both the six and nine shells^[1].

It can be seen from Figs. 4 and 5, as compression increases the total radial density increases and the radial density distribution of Δ 's increases sharply, but radial density of nucleons decreases

sharply. This suggests that the less dense outer part of the nucleus initially responds to the external load more readily than the inner part.

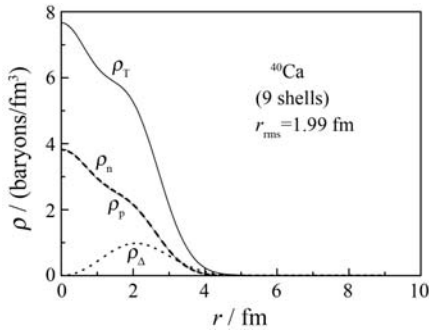


Fig. 5 Total ρ_T , proton ρ_p (dashed line), neutron ρ_n (solid line), and delta ρ_Δ (dotted line) radial density distributions for ^{40}Ca at point mass $r_{\text{rms}} = 1.99$ fm in a model space of nine major oscillator shells.

Clearly, the density in the interior rises relative to the interior density at equilibrium as one compresses the nucleus. This is in contrast to the behavior of the radial density on the outer-surface, where the radial density distribution is higher at equilibrium than the radial density when the static load is applied.

6 Conclusions

In the CSHF approximation the ground state properties of ^{40}Ca have been investigated at equilibrium and under static compression. In model space consisting of nine major oscillator shells with Δ resonances of nucleons restricted to ten Δ orbitals, the sensitivity of the results to the choice model space is examined.

The Δ degree of freedom is gradually populated as the nucleus is compressed. The number of Δ 's is decreased by increasing model space. Large amount of the compressive energy is delivered to create massive Δ in the nucleus. There is a significant reduction in the static compression modulus for RSC static compressions which is reduced by including the Δ excitations. The static compression modulus is decreased significantly by enlarge the

nucleon model space

Finally, if the static load force increases, then the compression of nucleus with nucleons only is less than the nucleus with nucleons and Δ 's.

References:

- [1] Abu-Sei'leek M H, Hasan M A. *Comm Theort Phys*, 2010, **54**(2): 339.
- [2] Deutchman P A. *Aust J Phys*, 1999, **52**(6): 955.
- [3] Terbert C M, Watts D P, Aguar P, *et al.* *Phys Rev Lett*, 2008, **100**(13): 132301.
- [4] Fernández de Córdoba P, Oset E, Vicente-Vacas M J. *Nucl Phys*, 1995, **A592**(4): 472.
- [5] Badalá A, Barbera R, Bonasera A, *et al.* *Phys Rev*, 1996, **C54**(5): R2138.
- [6] Mosel U, Metag V. *Nucl Phys News*, 1993, **3**: 25.
- [7] Xiong L, Wu Z G, Ko C M, *et al.* *Nucl Phys*, 1990, **A512**(4): 772.
- [8] Hofmann M, Mattiello R, Sorge H, *et al.* *Phys Rev*, 1995, **C51**(4): 2095.
- [9] Xing Yongzhong, Zheng Yuming, Pornrad S, *et al.* *Chin Phys Lett*, 2009, **26**(2): 022501.
- [10] Reid R V, *Ann Phys(N. Y.)*, 1968, **50**: 411.
- [11] Gari M, Niephaus G, Sommer B. *Phys Rev*, 1981, **C23**(1): 504.
- [12] Brandow B H. *Rev Mod Phys*, 1967, **39**(4): 771.
- [13] Bozzolo G, Vary J. *Phys Rev Lett*, 1984, **53**(9): 903.
- [14] Bozzolo G, Vary J. *Phys Rev*, 1985, **C31**(5): 1909.
- [15] Vary J, Yang S. *Phys Rev*, 1977, **C15**(4): 1545.
- [16] Lee S, Suzuki K. *Phys Lett*, 1980, **B91**: 79.
- [17] Suzuki K, Lee S. *Prog of Theor Phys*, 1980, **64**(6): 2091.
- [18] Kuo T, Wong S. *Lecture Notes in Physics*. Berlin: Springer, 1981, 248.
- [19] Abu-Sei'leek M H. *Comm Theort Phys*, 2011, **55**(1): 115.
- [20] Abu-Sei'leek M H. *Nuclear Physics Review*, 2010, **27**(4): 399.
- [21] Abu-Sei'leek M H, *Pramana-J of Phys*, 2011, **76**: 573.
- [22] Abu-Sei'leek M H. *International J of Pure and Applied Phys*, 2011, **7**(1): 73.
- [23] Saraceno M, Bozzolo J P, Miller H G. *Phys Rev*, 1988, **C37**(3): 1267.
- [24] Hasan M A, Köhler S H, Vary J P. *Phys Rev*, 1987, **C36**(5): 2649.
- [25] Hasan M A, Vary J P. *Phys Rev*, 1994, **C50**(1): 202.
- [26] Hasan M A, Vary J P. *Phys Rev*, 1996, **C54**(6): 3035.